Fine Structure of the Atrioventricular Node as Viewed in Serial Sections [1]

J. C. THAEMERT
The Congenital Heart Disease Research and Training Center, Hektoen Institute for Medical Research, 637 S. Wood Street, Chicago, Illinois 60612

ABSTRACT Atrioventricular nodal tissue obtained from a two-week-old mouse heart was fixed in osmium tetroxide, embedded in Epon 812, and serially sectioned for electron microscopy. From the study of electron micrographic montages of the first 620 serial sections of the posterior-inferior (tail) portion of the node, it was determined that many of the nodal cells are spindle-shaped and each has a single, centrally-placed, ellipsoidal nucleus. Other cells exhibit irregular surfaces with protrusions of variable dimensions and some are flattened. Most of the flattened cells are located in the peripheral borders of the posterior and lateral portions; irregularly-shaped cells occupy deeper positions in the tail of the node. Two cells, which are different from all others, reside in the peripheral border of the medial portion. They are contiguous with one another and globular in shape, each containing a single, centrally-placed, spherical nucleus. These two cells are sparsely endowed with myofilaments but contain many mitochondria. They may be pacemaker cells. Intercellular relationships among nodal cells exhibit a wide variety of complicated contact areas in addition to some rather simple contiguities of the lateral aspects of adjacent cells. No typical intercalated discs are present; however, junctional specializations between interdigitating protrusions of contiguous nodal cells do occur. Intimate contact between vesiculated nerve processes and nodal cells varies in extent from a profuse innervation in the posterior and lateral portions of the tail of the node to lack of contact with many of the cells in the medial and anterior portions. This pattern of innervation, in conjunction with the absence of maculae occludentes between cells of the posterior and lateral portions of the tail of the node but present between cells of the other portions, suggests that the medial and anterior areas are conductive and the posterior and lateral areas are regulative.

This report is the result of an analysis of electron micrographic montages of the first 620 serial sections of the posterior-inferior (tail) portion of the atrioventricular node of a mouse heart. It is concerned with the structural organization of the nodal cells, their interrelationships and the pattern of their innervation. Specific examples of nodal neuromuscular junctions in the first 115 serial sections of this series were reported previously in conjunction with three-dimensional illustrations (Thaemert, '70).

Electrophysiological evidence from experiments on the rabbit heart (Hoffman and Cranefield, '60), suggests that the normal delay in atrioventricular transmission occurs in the cells of the atrial or proximal portion of the atrioventricular node. Furthermore, it appears that the autonomic nervous system regulates the duration of this delay in relation to changes in the heart rate. This evidence also suggests that experimentally induced partial or complete atrioventricular block takes place in this portion of the node.

With the foregoing functional evidence in mind and because ultrastructural information about the atrioventricular node is fragmentary (DeFelice and Challice, '69; Hayashi, '62; James and Sherf, '68; Kawa-

[1] This investigation was supported by Research grants HL-07605 and NB-07299 from the National Institutes of Health, Bethesda, Maryland.

mura, '61; Kawamura and James, '71; Kawamura and Konishi, '67; Kim and Baba, '71; Melax and Leeson, '70; Maekawa, et al., '67; Merideth and Titus, '68; Thaemert, '70; Torri, '62; Viragh and Porte, '61), it seemed desirable to make a detailed ultrastructural study of the posterior-inferior (tail) portion of the atrioventricular node. This portion is the caudal part of the atrial or proximal portion of the node referred to by Hoffman and Cranefield ('60) and is small enough so that its entire transverse section can be studied with an electron microscope.

This interim report should assist in providing a morphological basis for explaining electrophysiological and pharmacological findings on the conduction system of the heart.

MATERIALS AND METHODS

The serial sections of this study were obtained from the same block of tissue used for the study reported previously (Thaemert, '70). Therefore, only a summary of the materials and methods used are presented.

The heart of a two-week-old mouse was perfused with a 1% buffered osmium tetroxide solution for approximately 20 minutes after which the heart was removed and sectioned transversely into three parts. The resulting slices were fixed for an additional four to five hours and subsequently embedded in Epon 812 after dehydration in ethanol. Serial sections 2 μ in thickness were obtained from the superior surface of the middle slice of the sectioned heart in a plane of section which was approximately parallel to the atrioventricular rings. These sections were stained with a polychrome stain and the components of the node followed from one section to the other with a light microscope until the posterio-inferior (tail) portion of the node was reached. At this time, excess tissue was trimmed away, leaving a block face measuring 1 mm^2. Two thousand serial sections were cut for electron microscopy. After being mounted on a supporting Parlodion membrane, each section was individually placed over a 0.2 mm $\times$ 0.5 mm slit in the center of a copper disc (specimen mount) and subsequently stained with uranyl acetate. Each section was approximately 100 $m\mu$ in thickness. Thinner sections were not sought because the danger of their loss was too great. The three-dimensional illustrations of nodal cells were produced from the reconstruction of the cellular profiles of every tenth serial section. Cellular profiles from the electron micrographic montages were traced on vellum paper. These tracings were over-laid with a grid-plane and subsequently redrawn on a perspective grid-plane. The tracings were then connected to one another in the most logical manner to form an illustration in perspective (Mitchell and Thaemert, '65).

OBSERVATIONS

The segment of the posterior-inferior (tail) portion of the node used in this study, is approximately 62 μ thick as determined from the measured thickness of the combined 620 serial sections (Peachey, '58). The other dimensions of this segment are approximately 156 μ from its posterior to its anterior borders and 76 μ from side to side (fig. 1). It is located in the subendocardial region of the atrioventricular septum, at the level of the confluence of the origins of the posterior and medial leaflets of the tricuspid valve and across the atrioventricular septum from the confluence of the septal origins of the two leaflets of the mitral valve. At the level of any one serial section, this portion of the node portrays approximately 155 sectioned nodal cell profiles. Most of them are sectioned transversely, a few obliquely and rarely, a portion of one in which the myofilaments appear in longitudinal section. These nodal cells occur in fascicles or bundles (fig. 1) which are separated by a network of capillaries, fibroblasts and nerve bundles in the intercellular spaces of the node. These fascicles change configuration as one studies the serial sections in sequence. This finding appears to be due to the changing positions of the meandering neurovascular elements.

Three-dimensional illustrations of nodal cells (figs. 2–19) represent the variety of sizes and shapes of nodal cells throughout the tail of the node. They range from small globular cells of the medial portion (figs. 12, 15) to large flattened cells in

the peripheral regions of the posterior-lateral portion (figs. 3–5). Many of the nodal cells are spindle-shaped and range from the relatively smooth-surfaced ones in the anterior (fig. 16) and central (fig. 11) portions of the tail of the node to those with irregular surfaces in the posterior-lateral portion (fig. 9). Despite the great variation in size and shape of nodal cells, they all contain ellipsoidal nuclei that vary in size with the volume of the cells except for two cells (fig. 13) which reside in the peripheral border of the medial portion of the tail of the node. Each of these two cells contains a spherical nucleus and its myofilaments are greatly reduced in number in relation to those of all other cells.

Intracellular components of the nodal cells, enclosed within the sarcolemma and an adherent basal lamina, comprise the nucleus, myofilaments, mitochondria, conical caps of sarcoplasm at each pole of the nucleus and islands of sarcoplasm positioned peripherally in the cell or interspersed among the myofilaments. Each ellipsoidal nucleus has a double membrane and contains from two to four spherical nucleoli averaging 0.8 μ in diameter. The granular chromatin is evenly distributed except for a variable number of spherical areas of increased density. The nucleus averages 5 μ in diameter and 10 μ long. Myofilaments are longitudinally disposed; however, since most cells are sectioned transversely, the organization of these myofilaments can be seen only in the few portions of cells in which some myofilaments are longitudinally sectioned (fig. 41). When the plane of section parallels the longitudinal axis of the myofilaments, A and I bands and Z discs can be detected. Due to the insertion of isolated accumulations of sarcoplasm and mitochondria between sparse strands of myofilaments, A and I bands and Z discs appear irregular and diminished within tenuous myofibrils. Therefore, striations may not be apparent in longitudinally-sectioned nodal cells when viewed with a light microscope (Lev, '68). The mitochondria are variably-shaped and elongated. They average 0.4 μ in diameter and 2 μ in length and are scattered rather uniformly throughout the nodal cells. In addition to mitochondria, conical caps and islands of sarcoplasm contain short segments of rough endoplasmic reticulum, free nucleoprotein and/or glycogen granules, multivesicular bodies, centrioles (figs. 39, 40), and occasional lysosomes. The vesicles and flattened cisternae of numerous unimpressive Golgi complexes are more prevalent in sarcoplasm surrounding the nucleus than in other areas of the cell. When the plane of section is proper, longitudinal elements of the sarcoplasmic reticulum are evident amongst the myofilaments (fig. 41). However, the distinctive transverse tubules of a T-system are not observed. Profiles of sarcolemma-lined culs-de-sac, which are prominent features in sections of nodal cells, may in some respects be comparable to the transverse tubules of the general myocardium. Many of them appear as profiles of large or small vacuoles, but when traced from one section to the next, some are continuous with the intercellular space through empty channels. Other vacuolar profiles contain either nerve processes (fig. 23) or protrusions (figs. 28–31) from adjacent cells which presumably have retracted. Most of the empty culs-de-sac are prominent in the peripheral cytoplasm beneath areas of intercellular contact (figs. 28–35); however, some are deep within the cells (figs. 25, 27). Some vacuolar profiles have no communication with the extra-cellular space and therefore appear to be true vacuoles.

Nodal cells do not possess the typical intercalated discs as seen in the general myocardium. There are, however, junctional specializations between interdigitating protrusions of contiguous nodal cells, namely, maculae adherentes (desmosomes), fasciae adherentes (wide areas of contiguity with increased density of the subsarcolemma) and maculae occludentes (gap or tight junctions). However, the interdigitating protrusions are not aligned like those of intercalated discs. Instead, they are highly irregular because the ends of most nodal cells do not meet. When two nodal cells do abut, the end of one cell invades the end of the other with an exchange of protrusions (figs. 36, 37). Many of the cells overlap each other so that the end of one cell may contact the side of another or just the ends may overlap (figs.

14, 28–35). In other instances, sides of adjacent cells may exchange small protrusions with one another (fig. 23). These intercellular relationships exhibit a wide variety of complicated contact areas in addition to some rather simple undifferentiated contiguities of the sarcolemmae of adjacent cells.

The foregoing descriptive comments of intercellular relationships are general in scope and apply in some degree to all regions. A notable exception is the complete absence of maculae occludentes between the cells of the posterior-lateral portion of the tail of the node and the peripherally-placed cells along its entire lateral edge. Nodal cells in these regions tend to be larger and more irregular in shape than cells in the other portions of the tail of the node. In addition they exhibit fewer areas of intercellular contact which exclude maculae occludentes. Maculae occludentes, on the other hand, are prevalent between the cells in the other regions of the tail of the node, (i.e., the central, medial and anterior portions). Here they exist as small circular plaques approximately 300 $m\mu$ in diameter. Rarely larger ones are present. The small maculae occludentes, which appear as points of "spot welding", are not positioned in a regular pattern. They are either grouped together in a relatively small area or widely scattered. However, they are more concentrated toward the ends of the nodal cells, especially where interdigitating protrusions are prevalent (figs. 28–34, 36). The middle third of the cell, which contains the nucleus, is usually free of maculae occludentes but occasionally they are present (fig. 23). There are, on the average, approximately 20 maculae occludentes per cell regardless of cell size or shape.

An extensive plexus of bundles of nerve processes is evident within the tail of the node. The cell bodies of supporting Schwann cells are situated at the intersections of the neural plexus (fig. 43). Schwann cells also cling to the surface of the tail of the node supporting bundles of nerve processes of varied sizes (fig. 42). The larger bundles divide to form smaller fascicles of vesiculated nerve processes that permeate the entire node. Each nodal cell, no matter in what part of the tail of the node, is at least within 100 $m\mu$ of one or more naked vesiculated nerve processes. Furthermore, intimate contact (neurocellular cleft less than 40 $m\mu$ and devoid of a basal lamina) between vesiculated nerve processes and nodal cells varies in extent. For example, there is a profuse innervation of the cells of the posterior-lateral portions of the tail of the node, where intimate neuromuscular contact is common (fig. 22). In contrast, there is a lack of nerve contact on many of the cells in the medial and anterior portions whereas the central region possesses cells with moderate contacts (figs. 23, 24). The majority of the varicosities of vesiculated nerve processes in contact with nodal cells, whether they are within culs-de-sac or within grooves of the external surface, are predominantly endowed with agranular vesicles (a, figs. 20, 22–24, 38, 43). However, in a few instances, a predominance of large granular vesicles is evident (a, fig. 40). Rarer still, are those varicosities that are endowed with an abundance of mitochondria (ne. fig. 20). This type of varicosity is similar to that reported as sensory in muscle spindles of skeletal muscle (Banker and Girvin, '71; Scalzi and Price, '71) and in the carotid body (Kondo, '71).

DISCUSSION

The present ultrastructural study was designed to bridge the gap that exists between light and electron microscopic studies on the conduction system of the heart. Light microscopic studies, due to the relatively low resolving power of the light microscope, have limited capacity to elucidate detailed morphological data even though large areas of tissue can be studied by employing the serial section method. On the other hand, electron microscopic studies that strive for the utmost in magnification and resolution require small and extremely thin serial sections which preclude the opportunity of studying relatively large areas of tissue. Therefore, by using a relatively low magnification and thicker serial sections mounted on supporting membranes to minimize section loss, the efforts put forth in the present investigation resulted in a clarification of the three-dimensional nature of nodal cells, their interrelation-

ships and their innervation within the entire cross-sectional area of the posterior-inferior (tail) portion of the atrioventricular node.

In several reviews of the voluminous light microscopic literature concerned with the structure of the atrioventricular node (Davies and Francis, ' 46; Lev, '68; Nomura, 52; Robb, '65; Truex, '61; Truex and Smythe, '65, '67), nodal cells were described as being fusiform, smaller than ordinary myocardial cells or like Purkinje cells. However, the precise structure and organization of nodal cells remain inconclusive.

With the advent of electron microscopy, a clearer concept emerged regarding atrioventricular nodal cell structure. Viragh and Porte ('61) were the first to exhibit electron micrographs of portions of nodal cells. Later, three comprehensive reports (Kawamura, '61; Torii, '62; Hayashi, '62) were published that revealed, to a higher degree, the fine structure of atrioventricular nodal cells in the dog, rabbit and cow hearts, respectively. These studies did not involve the three-dimensional technique and their electron micrographs, for the most part, showed only portions of nodal cells. However, their schematic drawings of groups of cells and Kawamura's illustration of his concept of the three-dimensional nature of nodal cells, correspond favorably to the three dimensional observations of the present study. Kawamura ('61), Torri ('62) and Hayashi ('62) described nodal cells as slender, small and irregular in shape. Similar observations were made in mouse, dog and monkey hearts by Maekawa et al. ('67), by Kawamura and Konishi ('67) in mouse hearts and by Merideth and Titus ('68) in human hearts.

James and Sherf ('68) on the basis of their ultrastructural observations of thin sections of the atrioventricular node in two human hearts, described four different types of cells in the atrioventricular node. First, round or ovoid cells with relatively smooth surfaces were considered to be identical to pacemaker cells in the sinus node. Second, slender and elongated cells were reported to resemble miniature working myocardial cells and the transitional cells of the sinus node. According to James and Sherf they are the most numerous in the atrioventricular node. Third, cells which resemble ordinary working myocardial cells were located only at the atrionodal margin. Fourth, there are cells identical to Purkinje cells, found only in the superficial layers of the node, DeFelice and Challice ('69), failed to describe the shapes of nodal cells in the rabbit heart but indicated their smaller diameters.

More recently, Melax and Leeson ('70), reported that the rat atrioventricular node is composed of modified cardiac muscle cells or Purkinje cells which are round or ovoid with relatively smooth surfaces and arranged in small groups of clusters. Kim and Baba ('71), found the nodal cells of the guinea pig atrioventricular node to be slender and irregularly shaped. Finally, Kawamura and James ('71), reported that the sinus and atrioventricular nodes of the monkey, bat and cow, contain nodal cells which are smaller than those in working myocardium and that "their shapes are highly variable being polygonal, branched, elongated or slender."

Three-dimensional evidence obtained in our study shows that the shape and size of atrioventricular nodal cells are both highly variable. These range from the small globular cells of the medial portion of the tail of the node to the large flattened cells at the periphery of the posterior and lateral portions. The two globular cells portrayed in figure 13 may be identical to the so-called pacemaker cells described by James and Sherf ('68). All of the remaining nodal cells, including the globular cells depicted in figures 12 and 15, appear to possess approximately the same complement and arrangement of intracellular organelles in proportion to their size despite an appreciable difference in size and shape. No Purkinje or working myocardial cells were observed within the tail of the atrioventricular node.

Unfortunately, little factual information is available regarding the relationship of the size, shape and association of nodal cells to the conduction velocity of the action potential within the atrioventricular node. It has been postulated that, in relation to their cross-sectional area, large cells conduct more rapidly than smaller ones (Katz, '48; Hodgkins, '64). Barr et al. ('65)

reported that maculae occludentes in frog atrial muscle are areas of low electrical resistance. Several investigators have attempted to correlate the fine structure of nodal cells and their interrelationships with the known normal delay in atrioventricular transmission. Hoffman and Cranefield ('60) reported this delay to take place in the atrioventricular node and assumed it to be due to the slow spread of the wave of excitation over a short distance. The ultrastructural study by Kawamura and James ('71), indicated that small nodal cells in the central portion of the atrioventricular node are connected to one another by maculae adherentes which lie scattered at irregular intervals; a few, small fasciae adherentes, the number and size of which correspond to the number and size of myofibrils; rare and small maculae occludentes; and large areas of undifferentiated contiguity. They attribute the reported scarcity of maculae occludentes and the small size of nodal cells as a possible explanation for the slower propagation of excitation within the node. This view was expressed also by Kim and Baba ('71). Other investigators (Torii, '61; Hayashi, '61; Kawamura, '61; James and Sherf, '68) gave a similar explanation for the slower propagation except that they observed no maculae occludentes between the nodal cells.

In a study of the atrioventricular nodal region of the rabbit heart DeFelice and Challice ('69) attempted to correlate the ultrastructure of nodal cells with their electrical properties. These authors reported that the delay in atrioventricular transmission is consistent with their findings of nodal cells with small diameters and sparsity or absence of maculae occludentes between them. They obtained their tissue samples from areas no closer than 0.5 mm to the site of the impaled microelectrodes. Kawamura and James ('71), criticized any correlative interpretation based on the nature and organization of nodal cells not directly impaled by the microelectrodes. The latter authors stated that "the shape and magnitude of the action potential vary considerably from fiber to fiber even within a small area in the node."

As noted above, a regional difference does exist in the presence or absence of maculae occludentes between the atrioventricular node cells of the mouse heart. The nodal cells within the posterior-lateral and lateral portions of the tail of the node, which are larger and more irregularly-shaped than cells in the other regions, are profusely invaded by vesiculated nerve processes and lack maculae occludentes. These findings suggest some sort of regulative function. However, the nodal cells of the other regions, have smaller cells, diminished innervation and the presence of maculae occludentes between them. These findings indicate such regions may be best suited for conduction.

ACKNOWLEDGMENTS

The author is indebted to Dr. Maurice Lev for his critical reading of this manuscript and to Richard Lark, Maryellen Kurek and Joan Ksycki for their excellent technical assistance and to Margo Shimizu for the three-dimensional illustrations.

LITERATURE CITED

Banker, B. Q., and J. P. Girvin 1971 The ultrastructural features of the mammalian muscle spindle. J. Neuropath. Exp. Neurol., *30:* 155–195.

Barr, L., M. M. Dewey and W. Berger 1965 Propagation of action potentials and the structure of the nexus in cardiac muscle. J. Gen. Physiol., *48:* 797–824.

Davies, F., and E. T. B. Francis 1946 The conduction system of the vertebrate heart. Biol. Rev., *21:* 173–188.

DeFelice, L. J., and C. E. Challice 1969 Anatomical and ultrastructural study of the electrophysiological atrioventricular node of the rabbit. Circulation Res., *24:* 457–474.

Hayashi, K. 1962 An electron microscope study on the conduction system of the cow heart. Jap. Circ. J., *26:* 765–842.

Hodgkin, A. L. 1964 The Conduction of the Nervous Impulse. Charles C Thomas, Springfield, Illinois.

Hoffman, B. F., and P. F. Cranefield 1960 Electrophysiology of the Heart. McGraw-Hill Book Co., Inc., New York, New York.

James, T. N., and L. Sherf 1968 Ultrastructure of the human atrioventricular node. Circulation, *37:* 1049–1070.

Katz, B. 1948 Electrical properties of the muscle fiber membrane. Proc. Roy. Soc. (London), *135:* 506–534.

Kawamura, K. 1961 Electron microscope studies on the cardiac conduction system of the dog. II. The sinoatrial and atrioventricular nodes. Jap. Circ., J., *25:* 973–1013.

Kawamura, K., and T. N. James 1971 Comparative ultrastructure of cellular junctions in working myocardium and the conduction sys-

tem under normal and pathological conditions. J. Mol. Cell. Card., *3:* 31–60.

Kawamura, K., and T. Konishi 1967 Ultrastructure of the cell junction of heart muscle with special reference to its functional significance in excitation conduction and to the concept of "disease of the intercalated disc." Jap. Circ. J., *31:* 1533–1543.

Kim, S., and N. Baba 1971 Atrioventricular node and Purkinje fibers of the guinea pig heart. Am. J. Anat., *132:* 339–354.

Kondo, H. 1971 An electronmicroscopic study on innervation of the carotid body of guinea pig. J. Ultrastruct. Res., *37:* 544–562.

Lev, M. 1968 The conduction system. In: Pathology of the Heart. S. E. Gould, ed. Third edition. Charles C Thomas, Springfield, Illinois, pp. 180–220.

Maekawa, M., Y. Nohara, K. Kawamura and K. Hayashi 1967 Electron microscope study of the conduction system in mammalian hearts. In: Electrophysiology and Ultrastructure of the Heart. T. Sano, V. Mizuhira and K. Matsuda, ed. Bunkodo Co., Ltd., Tokyo, Japan, pp. 41–54.

Melax, H., and T. S. Leeson 1970 Fine structure of the impulse-conducting system in rat heart. Canadian J. Zool., *48:* 837–839.

Merideth, J., and J. L. Titus 1968 The anatomic atrial connections between sinus and A-V node. Circulation, *37:* 566–579.

Mitchel, H. C., and J. C. Thaemert 1965 Three dimensions in fine structure. Science, *148:* 1480–1482.

Nomura, S. 1952 On the structure, distribution and innervation of the special heart muscle systems of the mouse. Cytological and Neurological Studies, *10:* 211–256.

Peachey, L. D. 1958 Thin sections. I. A study of section thickness and physical distortion produced during microtomy. J. Biophys. Biochem. Cytol., *4:* 233–242.

Robb, J. S. 1965 Comparative gross anatomy, histology and physiology of the atrioventricular connecting system. In: Comparative Basic Cardiology, Grune and Stratton, New York, pp. 349–432.

Scalzi, H. A., and H. M. Price 1971 The arrangement and sensory innervation of the intrafusal fibers in the feline muscle spindle. J. Ultrastruct. Res., *36:* 375–390.

Thaemert, J. C. 1970 Atrioventricular node innervation in ultrastructural three dimensions. Am. J. Anat., *128:* 239–264.

Torii, H. 1962 Electron microscope observation of the S-A and A-V nodes and Purkinje fibers of the rabbit. Jap. Circ. J., *26:* 39–77.

Truex, R. C. 1961 Comparative anatomy and functional considerations of the cardiac conduction system. In: The Specialized Tissues of the Heart. A. Paes De Carvalho, W. Carlos De Mello and B. F. Hoffman, eds. Elsevier Publ. Co., Amsterdam, pp. 22–38.

Truex, R. C., and M. Q. Smythe 1965 Comparative morphology of the cardiac conduction tissue in animals. Ann. N. Y. Acad. Sci., *127:* 19–33.

——— 1967 Reconstruction of the human atrioventricular node. Anat. Rec., *158:* 11–20.

Viragh, S., and A. Porte 1961 Structure fine du tissu vecteur dans le coeur de rat. Z. Zellforsch., *55:* 263–281.

——— 1961 Elements nerveux intracardiaques et innervation du myocarde. Etude au microscope electronique dans le coeur de rat. Z. Zellforsch., *55:* 282–296.

PLATE 1

EXPLANATION OF FIGURE

1 This low magnification montage of the entire transverse section of the posterior-inferior (tail)portion of the node is taken from section number 240. The plane of section is tilted in relation to the plane of the atrioventricular rings so that the top of the figure is slightly above the rings and the lower portion is slightly below them. The endocardium of the right atrium is to the left and out of the field of view; however, endothelium covering the proximal portion of the medial leaflet of the tricuspid valve can be identified in the lower left corner. A portion of the interatrial septum is in the upper right corner and a portion of the interventricular septum is in the lower right corner. The nodal cells exist in groups or fascicles. Clefts between the fascicles contain capillaries, fibroblasts and nerve bundles. The outlines on the over-leaf depict the fascicles at this level. The configuration of these facicles changes as they are followed through the series of sections. Numbers 2 to 19 on the over-leaf represent the figure numbers of the three-dimensional illustrations of representative nodal cells and indicate their relative positions within the tail of the node. Numbers 39 to 43 indicate the position of the nodal and Schwann cells of these respective figures. Stippled areas denote the relative location of all nodal cells possessing intimate contacts with vesiculated nerve processes within the 620 serial sections of this study. Notice that all the nodal cells within the posterior-lateral fascicle and most cells in the lateral fascicles are in intimate contact with vesiculated nerve processes whereas the remaining fascicles show diminished numbers of contacted cells. Approximately one-half of all nodal cells within the 620 sections are in intimate contact with vesiculated nerve processes. $\times$ 1,150.

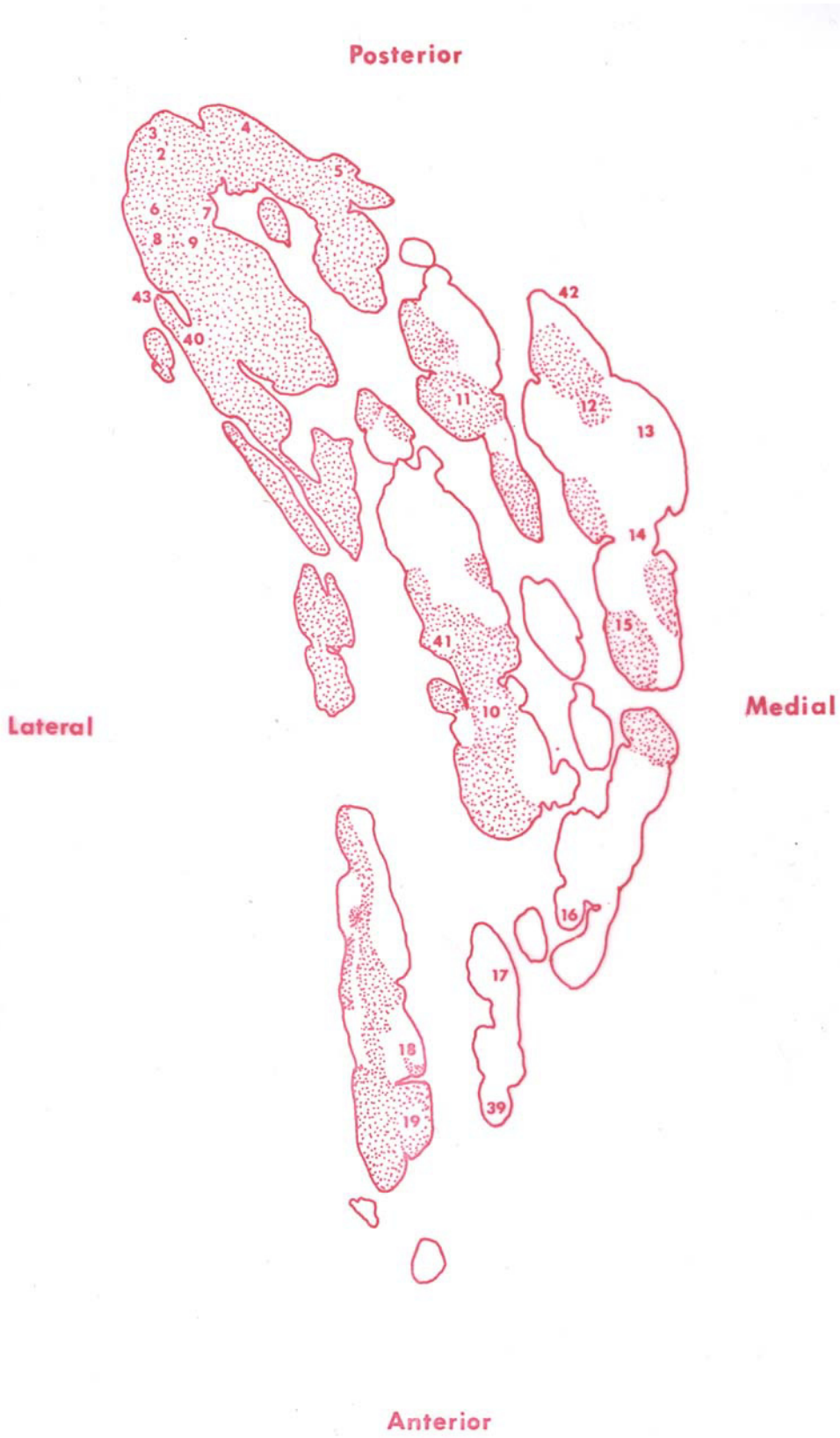
Posterior
Lateral
Medial
Anterior
3
2
4
5
6
7
8
9
43
40
42
11
12
13
14
15
41
10
16
17
18
19
39

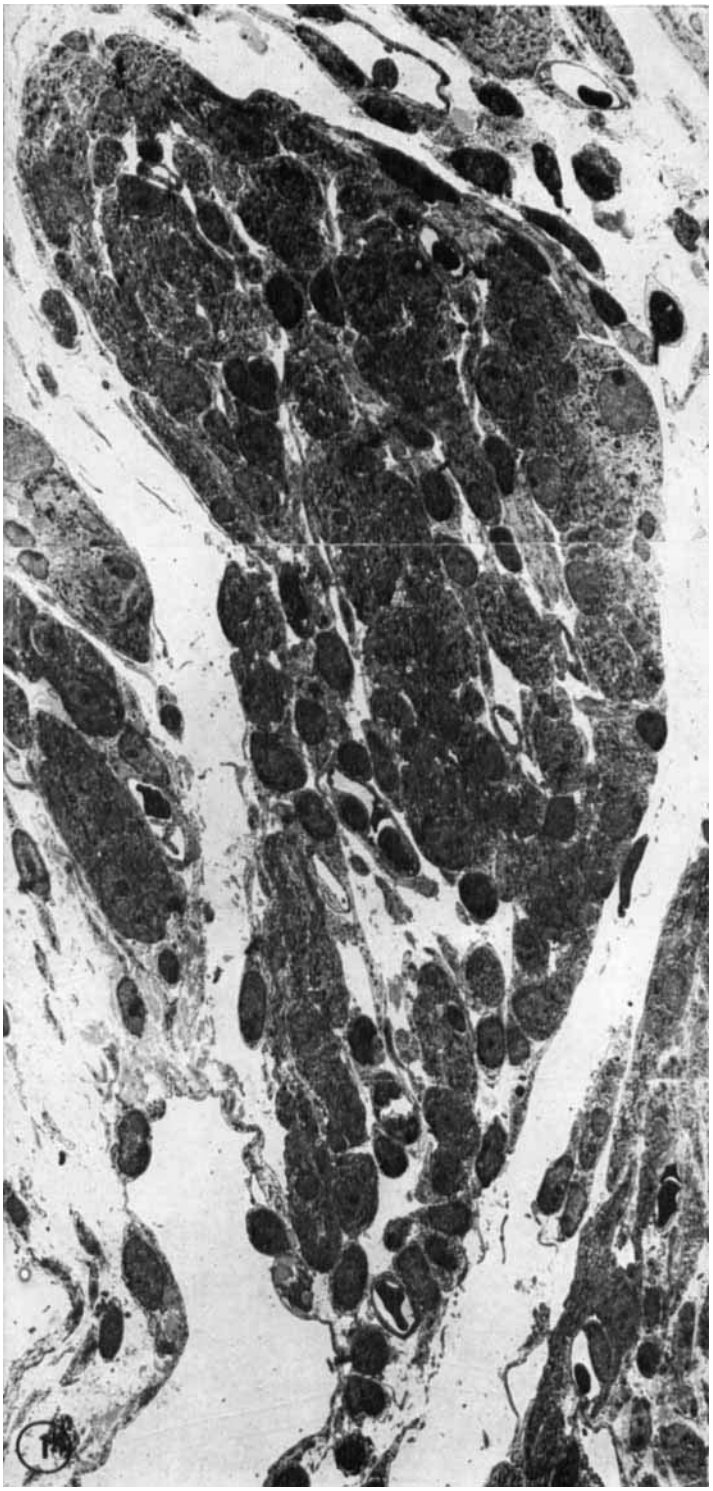

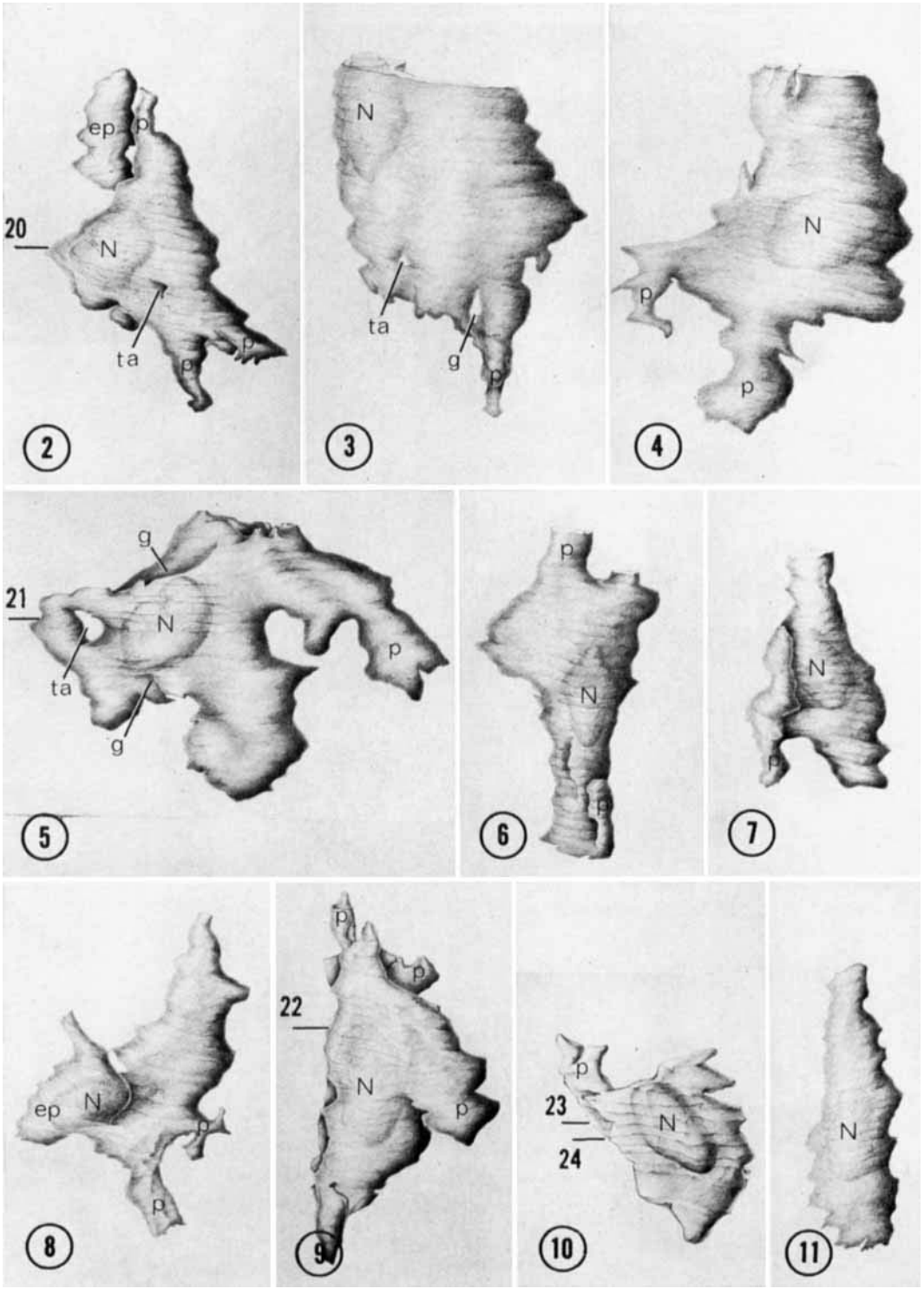
ep
p
20
N
ta
p
p
2
N
ta
g
p
3
N
p
p
4
g
21
N
ta
g
p
5
p
N
p
6
N
p
7
p
p
22
N
p
8
ep
N
p
p
9
p
23
24
N
10
N
11

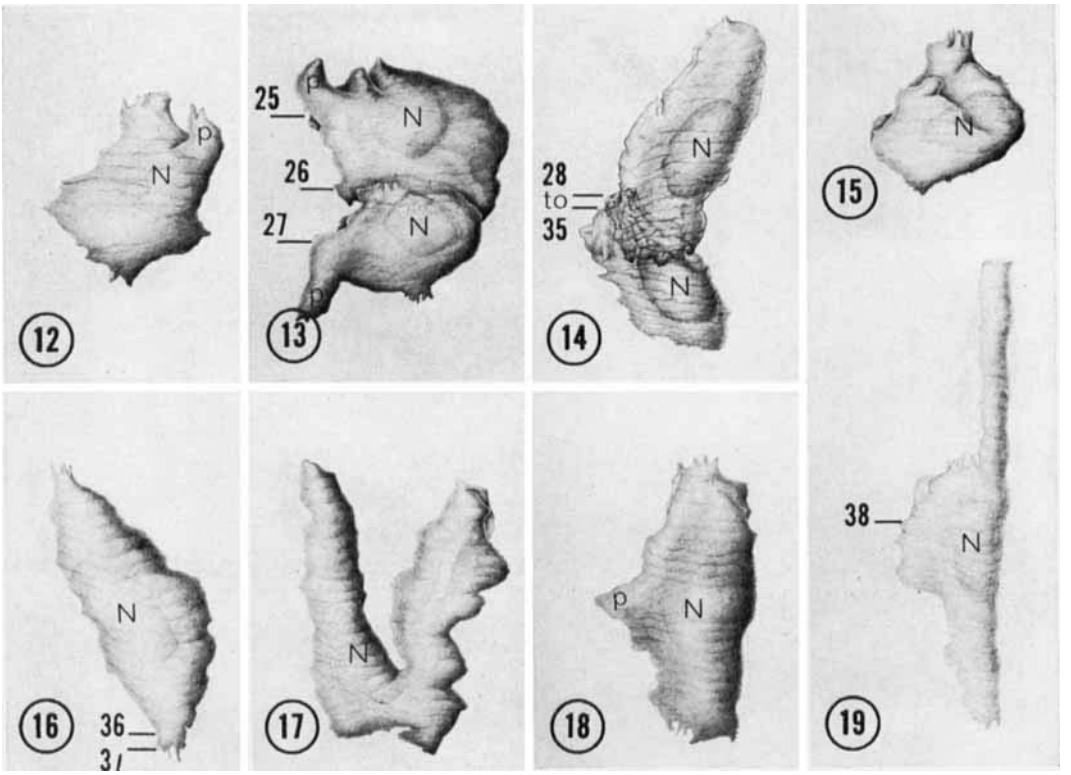

EXPLANATION OF FIGURES

2–19 Three-dimensional illustrations representative of the variability of size and shape of the nodal cells within the posterior-inferior (tail) portion of the node. Figure numbers indicate their position in the tail of the node in figure 1. Figures 2 to 9 depict nodal cells from the posterior-lateral fascicle. They tend to be more voluminous and irregularly shaped than cells in the other portions of the tail of the node. Peripherally-placed and flattened cells (figs. 3, 4, 5) form the surfaces of the posterior-lateral and some of the lateral fascicles but appear to be absent from the medial and anterior fascicles. Because of their flattened character and size, they cover a relatively large area. Such cells appear to be especially designed to permit the passage of nerve bundles by offering for this purpose, transcellular apertures (ta), grooves (g) and sometimes ragged, peripheral extensions or protrusions (p) which contact protrusions of adjacent cells to form passageways for both nerve bundles and capillaries. Interior cells within the posterior-lateral fascicle also possess similar properties but to a lesser degree as demonstrated by the transcellular aperture (ta) in fig. 2 and the variously-shaped protrusions (p) in figs. 2, 6, 7, 8 and 9. Expanded protrusions that are continuous with their respective cells through a constricted region are demonstrated in figure 2. Here an expanded protrusion (ep) extends to the left while in figure 8 another one extends to the bottom left. The cells of the central fascicles are represented by figs. 10 and 11. Cells within these fascicles are generally less voluminous and the irregularities of their surfaces are diminished when compared with cells of the posterior-lateral fascicle. Globular cells seem to be the most prominent within the medial fascicle (figs. 12, 13, 15). However, the cells in figure 14 are more elongate and represent cells of this type also present in this fascicle. The two unique cells in fig. 13 possess diameters greater than the other cells of this fascicle. Each cell is endowed with a spherical nucleus and a greatly reduced complement of myofilaments. Surface irregularities of the cells are also minimal within the fascicle. The anterior fascicles contain cells that tend to be more elongated and slender with relatively smooth surfaces, as in the central-anterior fascicles (figs. 16, 17) and in the lateral-anterior fascicle (figs. 18, 19). Some cells bend upon themselves (fig. 17). However, this type is seen infrequently. The horizontal lines in figs. 2, 5, 9, 10, 13, 14, 16 and 19 indicate the level of the electron micrographs in figs. 20 to 38. N, nucleus. × 1,500.

EXPLANATION OF FIGURE

20 The left two-thirds of the nodal cell illustrated in figure 2; level of section 184 indicated by the number 20. The profile of this unique cell is delineated by short arrows directed towards the surface of the cell. It is the only cell, whose cul-de-sac contained an exceptionally large nerve ending (ne) abundantly endowed with mitochondria. Several vesiculated nerve processes (a) occupy shallow grooves in the surface. This cell has moderate contact with adjacent cells. The contact is mostly of the undifferentiated variety but with some fasciae adherentes and maculae adherentes. N, nucleus; nu, nucleolus; d, dense chromatin; c, lumen of capillary; f, fibroblast; g, Golgi complex; mv, multivesicular body; b, nerve bundle; a, vesiculated nerve process; ne, nerve ending with mitochondria. × 10,000.

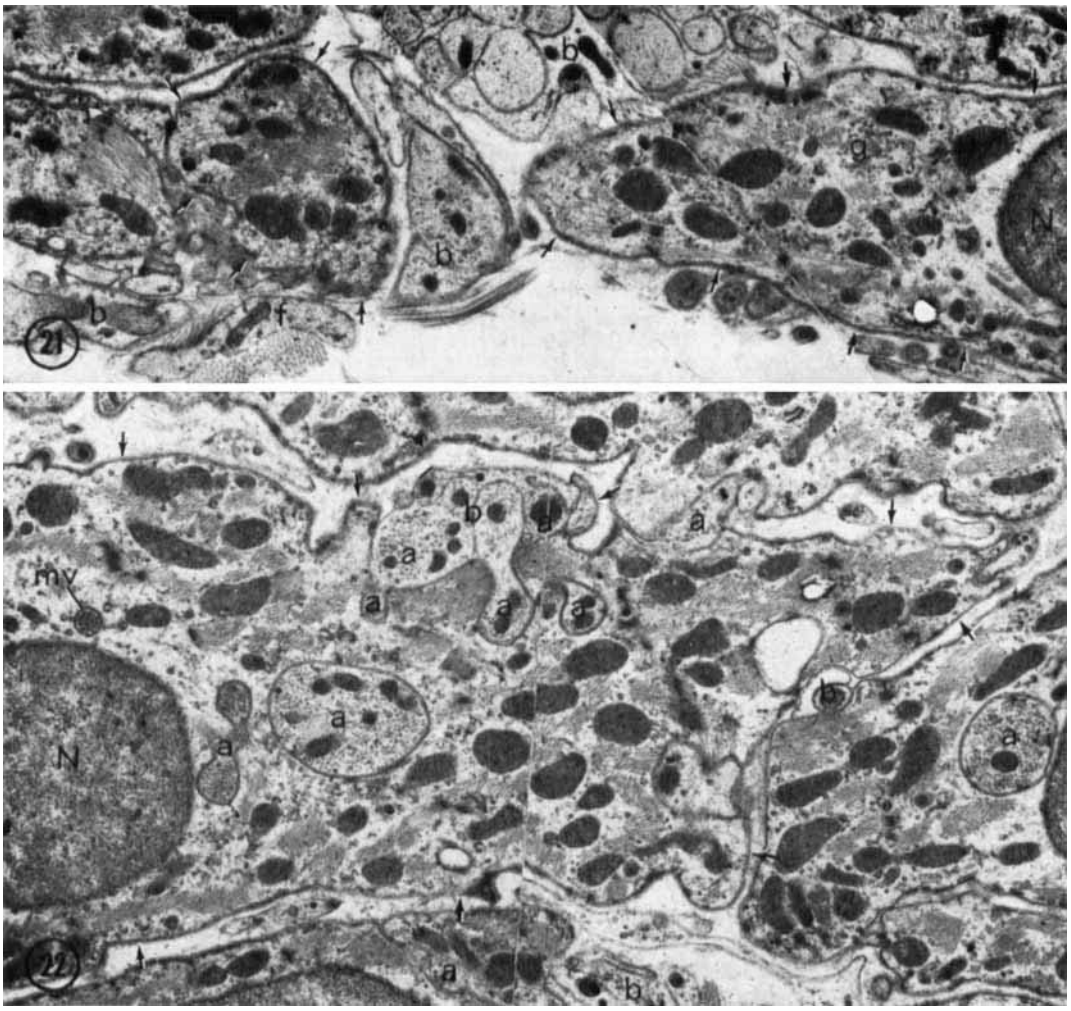

EXPLANATION OF FIGURES

21 The left one-fourth of the cross-sectional profile of the nodal cell illustrated in figure 5; level of section 301 indicated by number 21. The profile of this cell is delineated by short arrows directed toward its surface. This cell resides in the periphery of the tail of the node. Its outer surface is directed downward in this micrograph. The level of this section passes through the nucleus and the transcellular aperture. A nerve bundle (b) can be seen within the aperture. Intercellular contiguity between this cell and adjacent ones is minimal. The left end, which extends almost to the medial fascicle, makes contact through interdigitating protrusions with other cells and the right end has the same relationship with protrusions of the cell in figure 4. Fasciae adherentes and maculae adherentes do occur, but minimally, among the interdigitating protrusions. However, none are present at the level of this electron micrograph. Neuromuscular contiguity with this cell is meager. Vesiculated nerve processes make passing contact with the surface of this cell in only a few areas but none are shown in this micrograph. N, nucleus; b, nerve bundle; g, Golgi complex; f, fibroblastic process. × 10,000.

22 The right three-fourths of the cross sectional profile of the nodal cell illustrated in figure 9; level of section 352 indicated by number 22. The profile of this cell is delineated by short arrows directed toward its surface. This spindle-shaped nodal cell with several blunted lateral protrusions is situated centrally within the posterior-lateral fascicle and is more voluminous and irregularly shaped than spindle-shaped cells in other regions. It is profusely innervated by invading vesiculated nerve processes which ramify throughout the length of the cell within sarcolemma-lined culs-de-sac. The area of surface contact between nerve processes and the sarcolemma of this nodal cell is tremendous. Every serial section from section number 301 to 547 shows several vesiculated nerve processes within culs-de-sac. Surrounding cells also are profusely innervated but not as extensive as that of this cell. This nodal cell has moderate contact with adjacent cells, mostly of the undifferentiated variety. Some fasciae adherentes and maculae adherentes are present but maculae occludentes are absent. N, nucleus; b, nerve bundle; a, vesiculated nerve process; mv, multivesicular body. × 10,000.

PLATE 6

EXPLANATION OF FIGURES

23–24 These two electron micrographs portray the central cross-sectional profile of the nodal cell illustrated in figure 10. Their levels are indicated on the illustration by the numbers 23 and 24. The profiles of this cell are delineated by short arrows directed toward its surface. This cell is located anteriorly within the central fascicle and is one of the few nodal cells outside of the posterior-lateral fascicle that is innervated profusely by ramifying vesiculated nerve processes within sarcolemma-lined culs-de-sac inside the cell. The area of surface contact with nerve processes is considerable since every serial section between sections 231 to 339 shows vesiculated nerve processes within culs-de-sac. Good examples of agranular vesicles and the formation of varicosities (a) and attenuated intervaricose segments (s) of nerve processes can be seen in these two electron micrographs which are derived from sections that are approximately 800 $m\mu$ apart. The vacuole-appearing structures (v) to the right of the nucleus (fig. 23) are unoccupied extensions of the cul-de-sac that houses the varicosity (a) of the nerve process to the right of the nucleus in figure 24. This varicosity is continuous with the inter-varicose segment (s) in figure 23. The small varicosity (a) in the region just to the left and below the nucleus in figure 23 is continuous with the intervaricose segment (s) in the same location in figure 24. In addition, the larger varicosity (a) to the left of the nucleus is continuous with the nerve processes (a) just entering the nodal cell in the same region in figure 24. In its association with adjacent cells, this nodal cell exhibits large areas of undifferentiated contiguity in addition to fasciae adherentes, maculae adherentes and maculae occludentes (*) which are, in some cases, associated with interdigitating protrusions. Approximately 20 maculae occludentes are scattered irregularly over the surface of this cell. N, nucleus; nu, nucleolus; d, dense chromatin; g, Golgi complex; r, rough endoplasmic reticulum; mv, multivesicular body; v, vacuole-appearing structures; b, nerve bundle; a, varicosity of vesiculated nerve process; s, intervaricose segment of vesiculated nerve process. $\times$ 10,000.

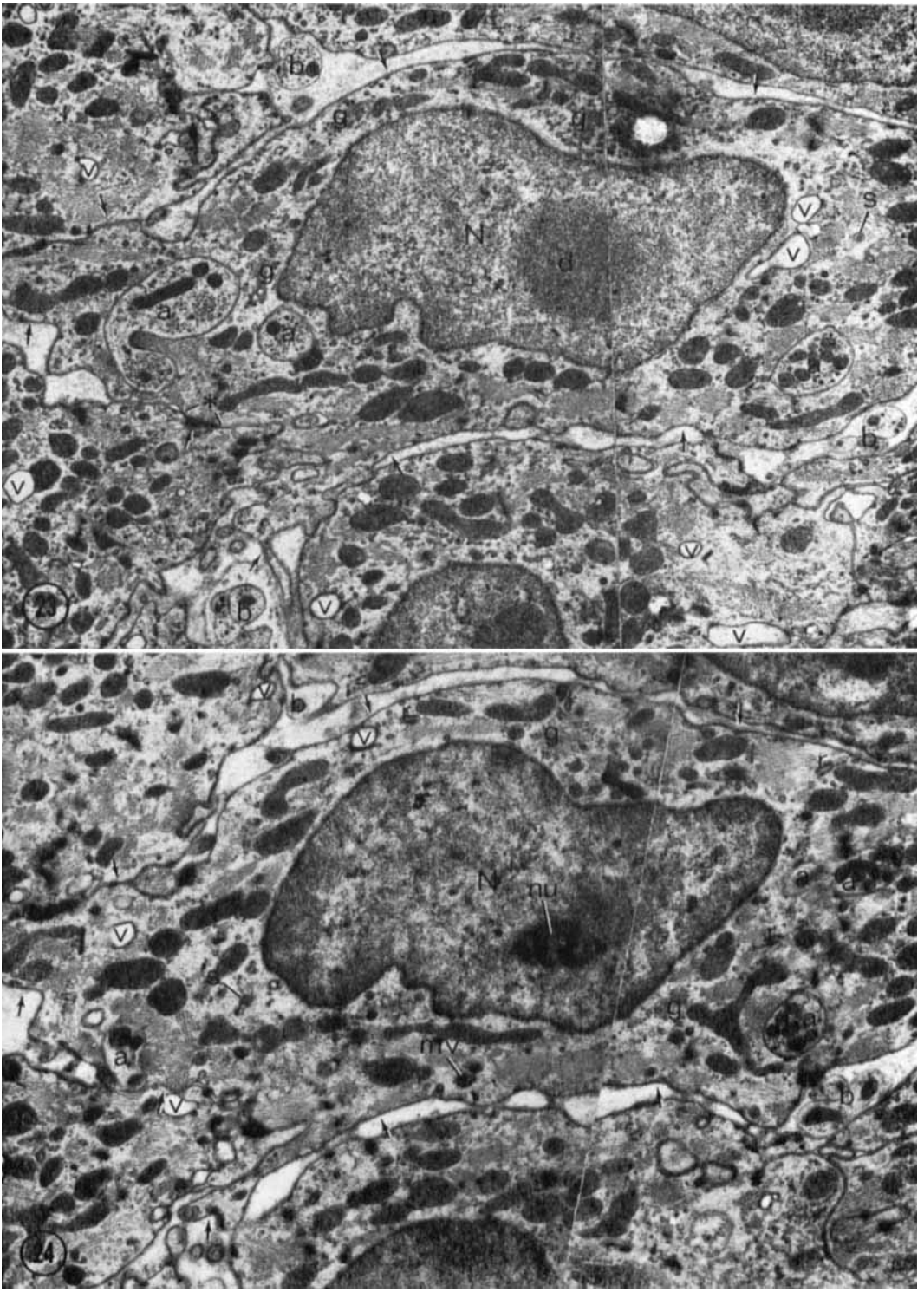
N
nu
mv
g
a
b
s
23
24

PLATE 7

EXPLANATION OF FIGURES

25–27 The entire cross-sectional profiles of the two contiguous nodal cells illustrated in figure 13. They are at the levels of sections 239, 292 and 315, respectively, and are indicated by numbers 25, 26 and 27. The profiles of these cells are delineated by short arrows directed toward the surface of the cells. These globular nodal cells reside in the periphery of the medial fascicle of the node. Their outer surfaces are directed upward in the electron micrographs. Contacts with vesiculated nerve processes are non-existent; however, several nerve processes approach to within 100 mμ of the surfaces of these two nodal cells. These cells differ from others in possessing spherical nuclei and sparse myofilaments. Each cell is penetrated by a relatively deep tortuous channel (v) that appears as a vacuole in the micrographs. The channel contains a laminated structure which actually is a protrusion (p) from the wall of the channel (fig. 25). Intercellular contiguity between these cells and adjacent ones consists of fasciae adherentes, maculae adherentes, maculae occludentes (*) and undifferentiated regions of contact. Seventeen maculae occludentes were counted on the surface of each cell. The upper portion (1c) of the lower cell is surrounded by the lower portion of the upper cell (fig. 26). N, nucleus; nu, nucleolus; v, vacuole appearing channel; b, nerve bundle; a, vesiculated nerve process; *, maculae occludentes; f, fibroblast; sc, Schwann cell; p, protrusions. $\times$ 5,000.

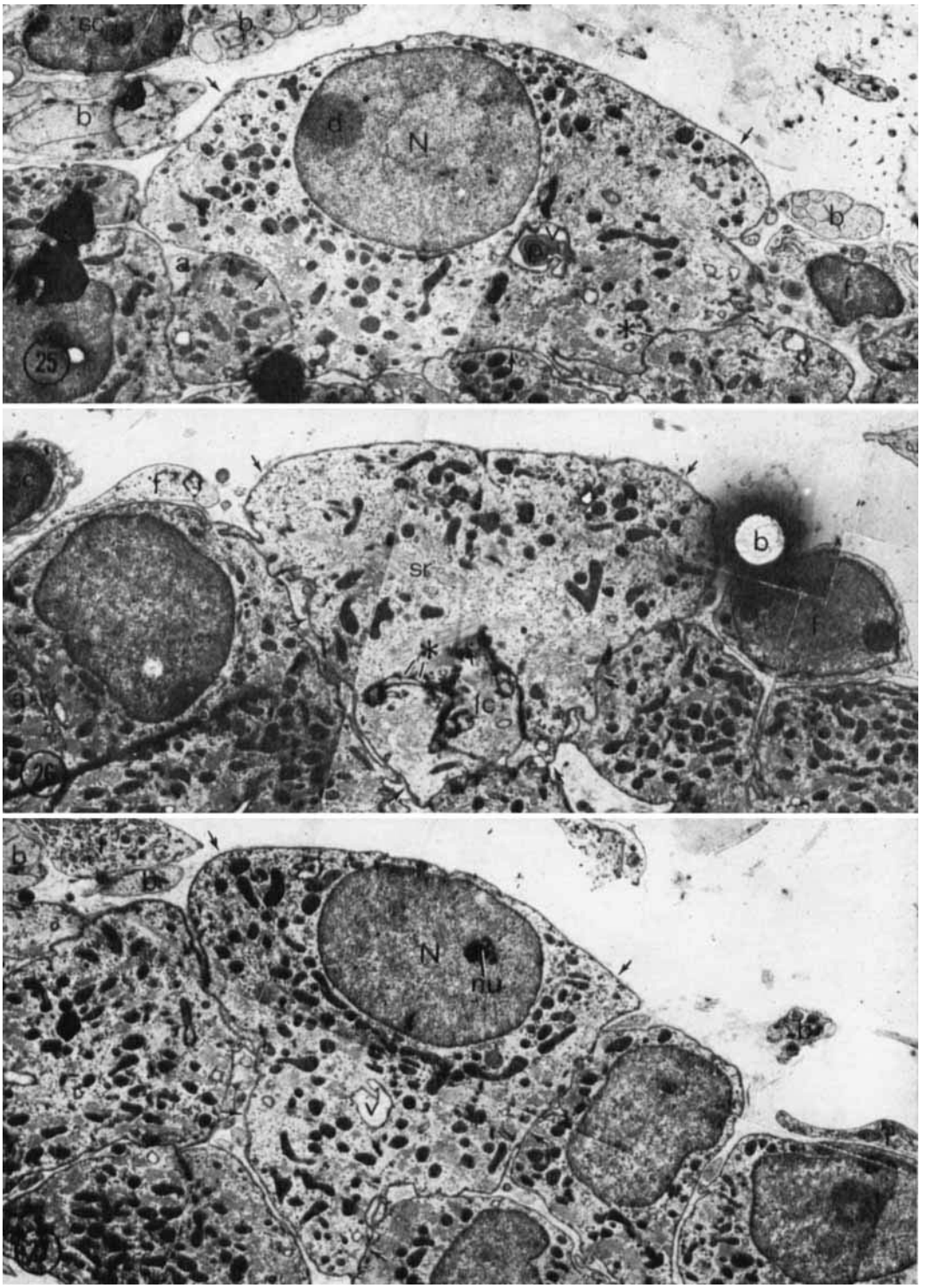
b
b
d
N
b
a
f
25
f
b
sr
lc
b
f
N
nu
v

PLATE 8

EXPLANATION OF FIGURES

28–35 These electron micrographs from eight consecutive serial sections portray a small representative region of the intercellular association of the two nodal cells illustrated in figure 14. This region is indicated on the illustration between the two horizontal lines. Small arrows delineate those surfaces of these two cells which are not contiguous with each other. The contiguous surfaces are indicated by small triangles; open triangles reside within the interdigitating protrusions of the cell on the right and solid triangles within those of the cell on the left. These cells exhibit regions of undifferentiated contiguity, fasciae adherentes, maculae adherentes and maculae occludentes (*). Most of the vacuole-appearing profiles possess continuity with the intercellular space. Those that can be shown to have such continuity, in a short series of sections such as this, are labeled (x) and those which are unoccupied extensions of culs-de-sac containing cellular protrusions, are labeled (z). These cells have no close contact with vesiculated nerve processes but nerve processes come within 100 mμ of their surfaces. $\times$ 10,000.

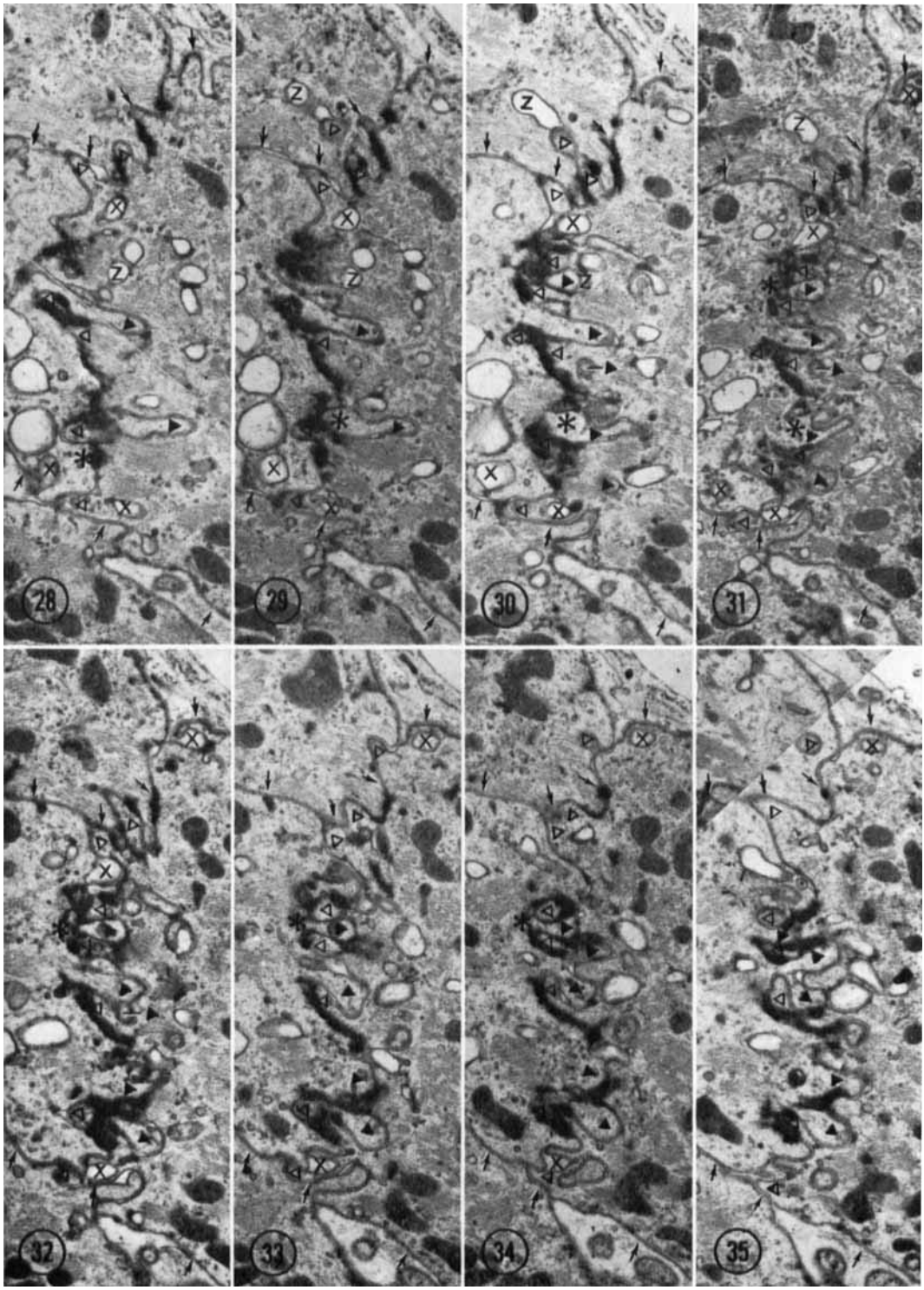
28
29
30
31
32
33
34
35

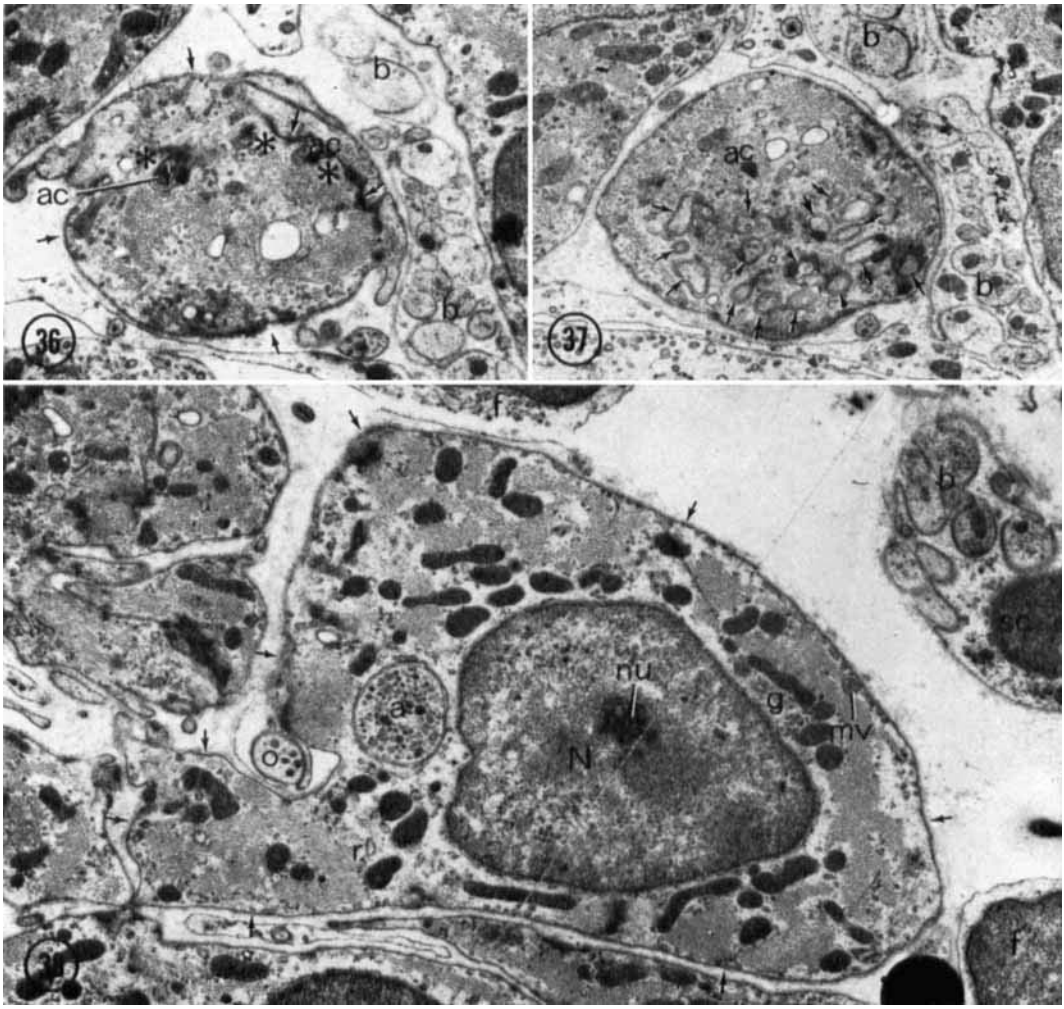

EXPLANATION OF FIGURES

36–37 These two electron micrographs, which come from sections approximately 2 μ apart, portray the entire cross-sectional profile of the lower end of the nodal cell illustrated in figure 16. They are at the levels of sections 256 and 275, respectively, and are indicated on the illustration by numbers 36 and 37. The profiles of this cell are delineated by short arrows directed toward the surface of the cell. This nodal cell shows only limited contact with another nodal cell (ac) which it meets end-to-end (fig. 36). Undifferentiated regions of contiguity, fasciae adherentes, maculae adherentes and maculae occludentes (*) are apparent. Twenty-six maculae occludentes are counted on the surface of this cell. In figure 37, all that remains are protrusions (arrows) residing in culs-de-sac of the other cell (ac) with only maculae adherentes and undifferentiated regions of contiguity. Contacts with vesiculated nerve processes are non-existent but several nerve processes approach to within 100 mμ of the surface of this cell. ac, cell with which that illustrated in figure 16 has end-to-end interrelationship; b, nerve bundle; *, maculae occludentes. × 10,000.

38 This electron micrograph portrays the entire cross-sectional profile of the nodal cell illustrated in figure 19. It is at the level of section 242 and is indicated on the illustration by the number 38. The profile of this cell is delineated by short arrows directed toward the surface of the cell. This elongated cell, with its swollen central region, is located in the anterior-lateral fascicle. It is one of only a few nodal cells possessing intimate contact with vesiculated nerve process having a predominance of large granular vesicles. This process (a) resides within a cul-de-sac near the nucleus and at the level of sections 235 to 239 it enters the nodal cell as an attenuated branch (not shown) of the Schwann cell-invested nerve process (o) which becomes varicose (a) shortly after entrance. This cell has moderate contiguity with adjacent cells, mostly of the undifferentiated variety but with some fasciae adherentes and maculae adherentes but no maculae occludentes. N, nucleus; nu, nucleolus; a, vesiculated nerve process; o, Schwann cell-invested nerve process; b, nerve bundle; sc, Schwann cell; g, Golgi complex; mv, multivesicular body; r, rough endoplasmic reticulum; f, fibroblast. × 10,000.

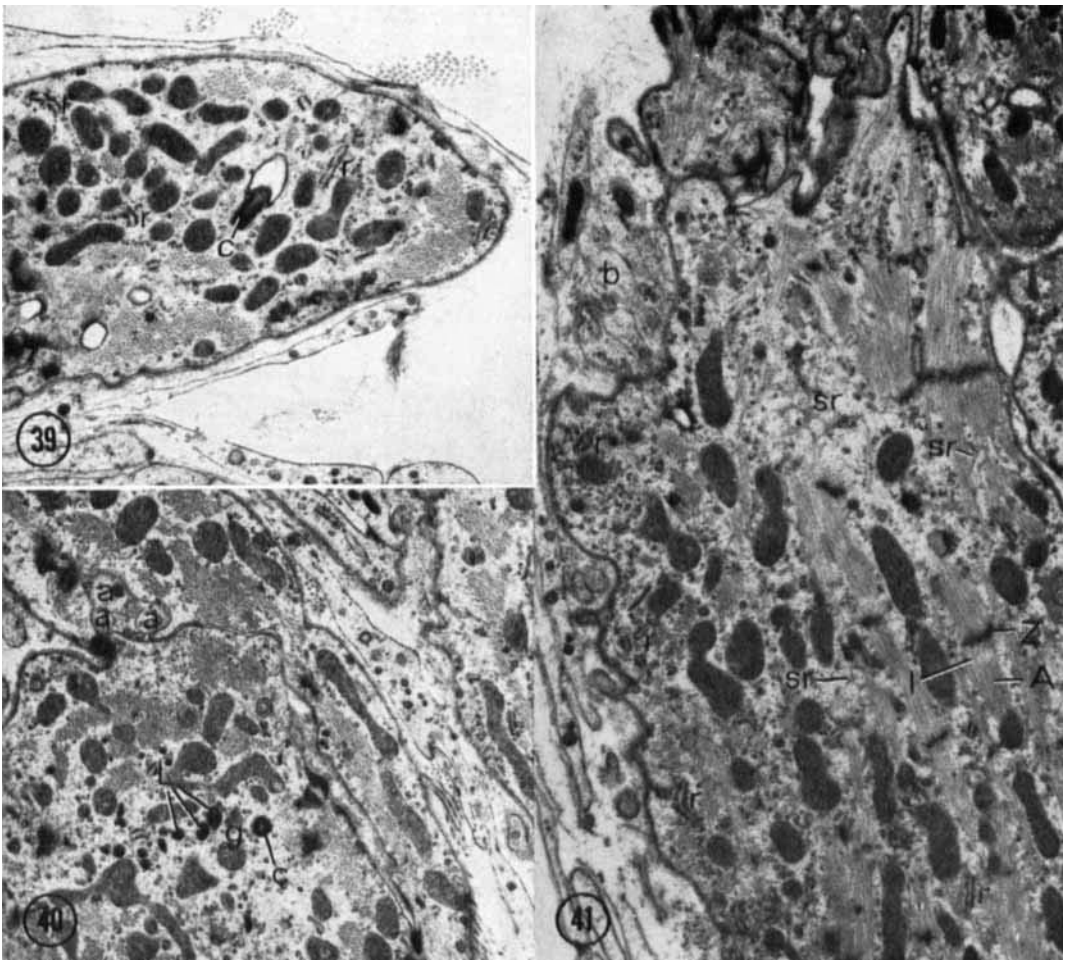

EXPLANATION OF FIGURES

39 This electron micrograph portrays a nodal cell containing a longitudinally sectioned centriole. (c). It protrudes into a vacuole and therefore appears to be an aborted cilium. Some centrioles do not have vacuoles associated with them. c, centriole; r, rough endoplasmic reticulum. × 10,000.

40 This electron micrograph portrays a nodal cell containing a transversely sectioned centriole (c). a, vesiculated nerve processes which are part of a small nerve bundle making contact with nodal cells; L, lyosomes; g, Golgi complex × 10,000.

41 This electron micrograph portrays a nodal cell in which myofilaments appear in longitudinal section. Notice that myofibrillar formation is diminished and irregular. Z, Z-disc; A, A-band; I, I-band; sr, sarcoplasmic reticulum; r, rough endoplasmic reticulum; b, nerve bundle. × 10,000.

PLATE 11

EXPLANATION OF FIGURES

42 This electron micrograph portrays the cell body of a Schwann cell (sc) situated on the surface of the tail of the node where it supports a nerve bundle (b) of variously-sized nerve processes. r, short segments of rough endoplasmic reticulum; f, fibroblast. × 10,000.

43 This electron micrograph portrays the cell body of a Schwann cell (sc) situated on the surface of the tail of the node at a site of entrance of a branch of the peripheral nerve plexus into the substance of the tail of the node. In this position the Schwann cell is at the intersection of the plexus and is supporting bundles of both vesiculated and non-vesiculated nerve processes (b). g, Golgi complex; f, fibroblast; a, vesiculated nerve process in close contact with the surfaces of two nodal cells. × 10,000.

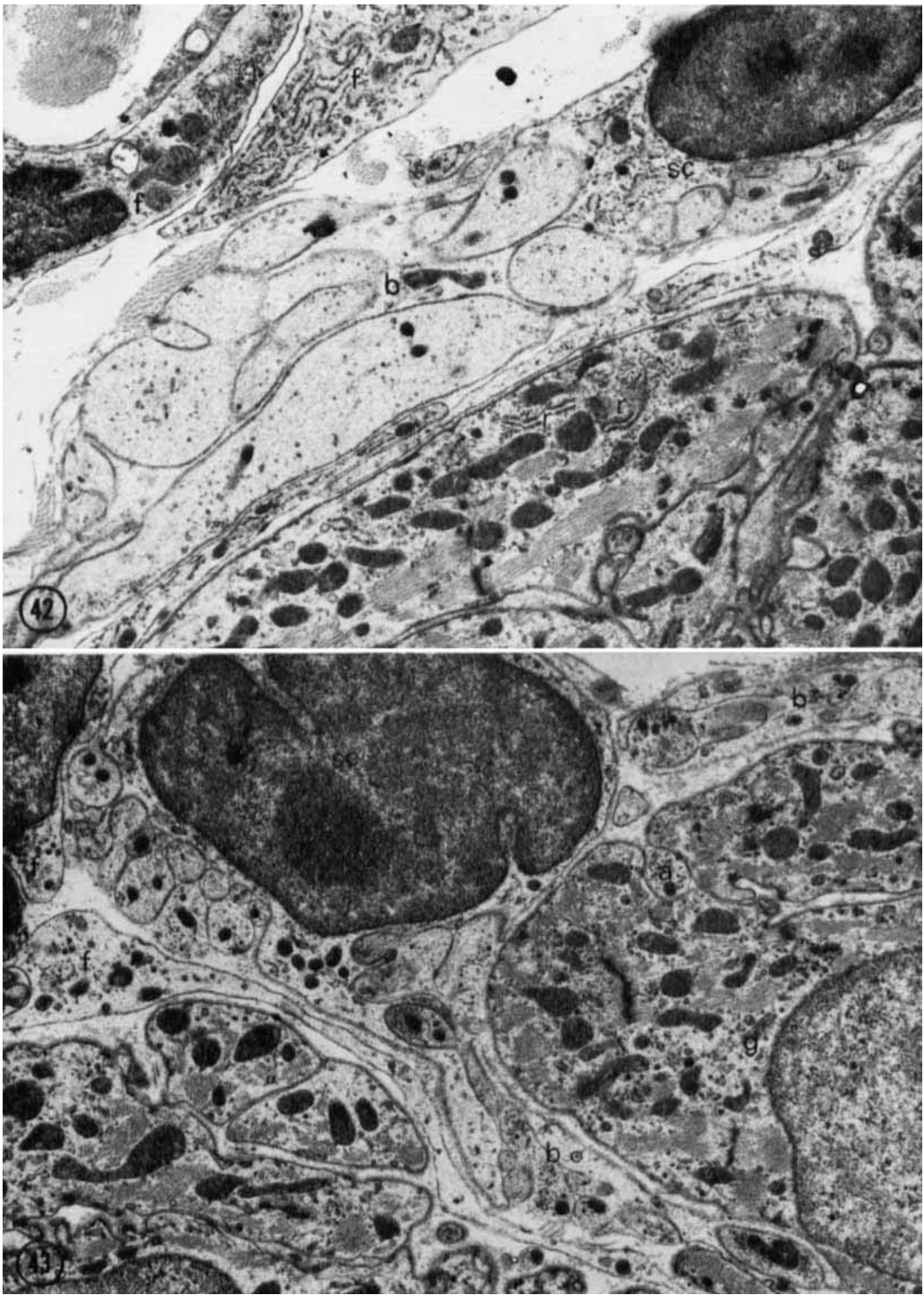
f
f
sc
b
r
r
42
sc
b
a
f
f
g
b
43